Cancer Research

Cathepsin B inhibition limits bone metastasis in breast cancer

Nimali P Withana, Galia Blum, Mansoureh Sameni, et al.

Cancer Res Published OnlineFirst January 19, 2012.

Cathepsin B inhibition limits bone metastasis in breast cancer

Nimali P Withana[1,2], Galia Blum[4,5], Mansoureh Sameni[6], Clare Slaney[1], Arulselvi Anbalagan[6], Mary B Olive[7], Bradley N Bidwell [1,3], Laura Edgington[4], Ling Wang[4], Kamiar Moin[6,7], Bonnie F Sloane[6,7], Robin L Anderson[1,2], Matthew S Bogyo[4,8] , Belinda S Parker [1,3]

[1]Research Division, Peter MacCallum Cancer Centre, East Melbourne, Australia 3002. [2]Department of Pathology and [3]Department of Biochemistry and Molecular Biology, University of Melbourne, Parkville, Australia 3010. [4]Department of Pathology, Stanford University, School of Medicine, Stanford, CA 94305, USA. [5]Institute of Drug Research, The School of Pharmacy, Faculty of Medicine, Campus Ein Karem, The Hebrew University Jerusalem, Israel, 91120. [6]Department of Pharmacology, Wayne State University, School of Medicine, 540 East Canfield, Detroit. MI 48201, USA. [7]Barbara Ann Karmanos Cancer Institute, Wayne State University, Detroit, MI 48201, USA. [8]Department of Microbiology and Immunology, Stanford University, School of Medicine, Stanford, CA 94305, USA.

Running Title: Cathepsin B inhibition reduces bone metastasis

Key words: breast cancer, bone metastasis, cathepsin B, cysteine protease, CA-074

Financial Support: National Health and Medical Research Council Australia (NHMRC) Project Grant (BSP, RLA, MSB), NHMRC CDA1 Fellowship (BSP), NIH/National Cancer Institute Grant ROI CA90291 (RLA), National Breast Cancer Foundation of Australia Fellowship (RLA), NIH R01 CA131990 (BFS).

Corresponding Author: Dr Belinda S Parker, Research Division, Peter MacCallum Cancer Centre St Andrews Place, East Melbourne, Victoria, 3002, Australia. Ph: +61 3 96561285, Fax: +61 3 96561411, Email: belinda.parker@petermac.org

Word Count: 4999

Total Figures: 6

Abstract:

Metastasis to bone is a major cause of morbidity in breast cancer patients, emphasizing the importance of identifying molecular drivers of bone metastasis for new therapeutic targets. The endogenous cysteine cathepsin inhibitor stefin A is a suppressor of breast cancer metastasis to bone that is co-expressed with cathepsin B in bone metastases. In this study, we used the immunocompetent 4T1.2 model of breast cancer which exhibits spontaneous bone metastasis to evaluate the function and therapeutic targeting potential of cathepsin B in this setting of advanced disease. Cathepsin B abundancy in the model mimicked human disease, both at the level of primary tumors and matched spinal metastases. RNAi-mediated knockdown of cathepsin B in tumor cells reduced collagen I degradation *in vitro* and bone metastasis *in vivo*. Similarly, intraperitoneal administration of the highly selective cathepsin B inhibitor CA-074 reduced metastasis in tumor-bearing animals, a reduction that was not reproduced by the broad spectrum cysteine cathepsin inhibitor JPM-OEt. Notably, metastasis suppression by CA-074 was maintained in a late treatment setting, pointing to a role in metastatic outgrowth. Together, our findings established a pro-metastatic role for cathepsin B in distant metastasis and illustrated the therapeutic benefits of its selective inhibition *in vivo*.

Precis:

This study offers a preclinical proof of concept for a therapeutic strategy to block metastasis of breast cancer cells to bone, a common feature of malignant progression in breast cancer patients with few effective treatment options at present.

Introduction:

Early detection of breast cancer has increased the 5-year survival rate to over 85%. However, progression to metastatic disease in tissues such as lung and bone reduces the survival rate to 23% due to limited curative treatments available (1). Hence, it is important to determine the mechanisms involved in primary tumor cell invasion and spread to distant sites such as bone, to allow identification of molecular targets for new therapies.

Proteases contribute to tumor cell invasion and angiogenesis and are commonly associated with metastasis. It is now recognized that cysteine proteases play pivotal roles in cancer progression. There are eleven members in the human cysteine cathepsin family (cathepsins B, C, H, F, K, L, O, S, V, W X/Z) and nineteen in mouse (2). In normal cells, cysteine cathepsins are expressed primarily in lysosomes and have roles in antigen presentation, apoptosis, autophagy and cellular homeostasis (3-6). Secreted cathepsin K is well documented to contribute to bone resorption and remodelling (7). In cancer, the cellular localization of lysosomal cysteine cathepsins is often altered. Intracellular, cell surface and secreted cysteine cathepsins are involved in distinct tumorigenic processes *in vivo*, such as angiogenesis, invasion through extracellular matrices and metastasis (8-10).

Of the cysteine cathepsins, B and L have been implicated most in tumorigenesis (9, 11, 12). Cathepsins B and L are prognostic markers in several types of cancer, including breast, with increased primary tumor expression associated with poor outcome (13-15). In the PyMT-induced transgenic mammary carcinoma model, ablation of cathepsin B reduces and delays lung metastasis (16), while increased expression of cathepsin B enhances metastasis in the same model (17). The pro-metastatic role of cysteine cathepsins has also been demonstrated in a multistage transgenic model of pancreatic cancer. Treatment of mice with a broad spectrum cysteine cathepsin inhibitor decreases tumor vascularization

and invasion (18), an effect that is enhanced when cysteine cathepsin inhibitors are combined with chemotherapy (19). Taken together, these data indicate that cysteine cathepsins have important roles in metastasis. Since bone is the most common site of distant metastasis in breast cancer patients, determining the roles of cysteine cathepsins in bone metastasis is crucial.

Our previous studies support a role for cysteine cathepsins in bone metastasis (20). Using our unique 4T1.2 syngeneic model of spontaneous bone metastasis (21), we identified the endogenous cysteine cathepsin inhibitor stefin A as a metastasis suppressor. Tumor cell stefin A significantly reduced pulmonary and bone metastasis in the murine model and was an independent predictor of good prognosis in a cohort of 142 breast cancer patients (20). Of the cysteine cathepsins, cathepsin B was co-expressed with stefin A in primary tumors and metastases, suggesting that stefin A suppressed metastasis via inhibition of cathepsin B. This was supportive of previous studies that demonstrate that a shift in equilibrium between cathepsin B and its endogenous inhibitor stefin A predicts poor survival outcomes (22, 23).

In this study, we utilized our 4T1.2 model to demonstrate a critical function of cathepsin B in breast cancer metastasis to bone. Molecular suppression and selective therapeutic inhibition of cathepsin B significantly reduces pulmonary and bone metastasis. This study provides evidence that cathepsin B is a potential therapeutic target for treatment of breast cancer patients with metastatic disease.

Methods:

Immunohistochemistry (IHC). All tissues were fixed in 10% neutral buffered formalin for 24 hours, bones decalcified in 20% EDTA, pH 8.0 and embedded in paraffin. Archived human material was utilized where previous informed consent was obtained from all patients. Citrate buffer (10mM, pH 6.0) high temperature and pressure antigen retrieval was required for human tissues and IHC was then carried out on tissue sections as described previously (20).

Cell maintenance. The 4T1.2 lines (21) were derived in our laboratory from the parental mouse 4T1 mammary tumor cell line. The 4T1 cell line was derived by Fred Miller that, along with a series of other lines, was originally derived from a spontaneous mammary tumor in Balb/c mice. Cells were maintained in alpha-modified eagle medium (α-MEM) supplemented with 5% fetal bovine serum (FBS, JRH Biosciences, KA, USA) and cultured at 37°C in an atmosphere of 5% CO_2 for no more than 4 weeks.

Generation of stable cathepsin B knockdown and base vector control clones. Short hairpin (sh)RNA for cathepsin B (5'-GGATGACCTGATTAACTA-3') along with control shRNA (5'-AGTACTGCTTACGATACGG – 3') lacking a murine gene target were inserted into pRetroSuper retroviral expression plasmids (Oligoengine, WA, USA) prior to transfection into PT67 retroviral packaging cells using Lipofectamine 2000 (Invitrogen, CA, USA) and infection of 4T1.2 target cells. Stably transduced cells were selected with puromycin (8μg/mL). Single cells were sorted (FACSVantage-Diva, BD Biosciences, Franklin Lakes, NJ, USA), expanded in culture and analyzed for gene expression by real-time RT-PCR and immunoblotting. Four clones of tumor cells containing control base vector (4T1.2 BV) or cathepsin B specific hairpins (4T1.2 CTSB kd) were pooled for subsequent analysis.

Immunocytochemistry. 4T1.2, 4T1.2 BV and CTSB kd cells were grown on uncoated glass coverslips for 24 hours, fixed in 3.7% cold paraformaldehyde and then blocked in PBS containing 2 mg/ml BSA. Cells were then incubated overnight at 4°C with primary antibody, rabbit anti-human cathepsin B (24). Cathepsin B expression was detected with FITC Alexa Fluor 488 donkey anti-rabbit secondary antibody (Invitrogen, CA, USA) and imaged on a Zeiss LSM 510 META confocal microscope.

Live cell proteolysis assay. Proteolysis was measured according to previously published procedures (26, 27). Briefly, glass coverslips were coated with 50 µl of 25 mg/ml quenched fluorescent substrate DQ-collagen IV (Invitrogen, CA, USA) mixed with reconstituted basement membrane (rBM) Cultrex (Trevigen, MD, USA). For collagen I, plastic coverslips were coated with 100 µl of 25 mg/ml DQ-collagen I (Invitrogen, CA, USA) mixed with collagen I (Advanced BioMatrix, CA, USA). The ratio of quenched fluorescent components to non-fluorescent components was 1:40 for all experiments. Cells were seeded at a density of 5000 cells per coverslip and cultured in serum-containing medium for 48 hours. Activity based probe GB123 (1 µM) was added to the media 16-18 hours prior to imaging. Fluorescence was then observed by confocal microscopy on a Zeiss LSM 510 using a 40x water immersion lens. Cell lysates labeled with GB123 were separated by SDS-PAGE and visualized by scanning with a typhoon flatbed laser scanner (excitation/emission 633/680nm). For inhibitor studies, the highly selective cathepsin B inhibitor CA-074 was synthesized and purified in the Bogyo laboratory, CA, USA and used at 20 µM (in DMSO vehicle) and replenished after 24 hours. The fluorescent GB123 probe was produced as described previously (28).

***In vivo* metastasis assay.** Cells (1 x 10^5) in PBS were mixed 1:1 with Matrigel (BD Biosciences, Franklin Lakes, NJ, USA) and injected orthotopically into the 4th mammary gland of 6 week-old female

Balb/c mice (Walter and Eliza Hall Institute, Parkville, Australia), 20 mice per group. Tumor volume was calculated as: Volume = (Length(mm) x Width(mm)^2/2). Mice were injected (intra peritoneal, 200µL/20g mouse) daily with 50mg/kg JPM-OEt (Drug Synthesis and Chemistry Branch, Division of Cancer Treatment and Diagnosis, National Cancer Institute, MD, USA), CA074 or vehicle (Saline/5% DMSO), three days post tumor inoculation. After 30 days, all mice were culled upon any signs of distress due to metastasis by inhalation overdose and the organs resected. Tumor burden was measured by quantitative real time PCR (RT-QPCR) as previously validated and published (Eckhardt et al., 2005) and 3 mice out of 20 were randomly selected for histology. For RT-QPCR, multiplex amplification of hygromycin/vimentin was used to measure tumor cell DNA signal (hygromycinR) relative to a marker present in all cells (vimentin). Reactions were performed on an ABI Prism 7000 thermocycler. Relative tumor burden (RTB) in an organ was calculated by: RTB = 10000 / ($2^{\Delta CT}$), where ΔCT = CT (Hygromycin) – CT (Vimentin). Late treatment studies were conducted as above but with resection of primary tumors at day 15 (~0.3g) and treatment of mice with CA-074 or vehicle daily beginning at day 29 and until signs of metastasis were evident in either group, at which point all mice were culled and assessed for metastatic burden. Any mice with primary tumor re-growth were excluded from the study. Mouse studies were conducted only after approval by the Peter MacCallum Ethics Review Board.

Non-invasive imaging of 4T1.2 tumor burden mice. 4T1.2 cells were injected into the 4th mammary fat pad of 6 week old Balb/c mice followed 3 days later by daily intra-peritoneal injections of CA-074 (50mg/kg) or vehicle (5% DMSO/Saline.) Probes (25 nmol GB123 or 2 nmol osteosense750, VisEn Imaging, Inc.) were administered through the tail vain in a solution of 67% DMSO, 33% PBS in 100µl final volume, 24 hours prior to imaging. Mice were then anesthetized with 3% isoflurane, and tomographic images taken using the FMT2500 imaging system, using the 680nm or 750nm channels. All animal experiments were approved by the Stanford Administrative Panel on Animal Care.

Statistical Analysis of Data. Statistics were performed using the data analysis package within GraphPad Prism 5.0 for Windows (GraphPad Software, San Diego, CA, USA). Unless otherwise stated, tests comparing two means are a Student's t-test, with equal variance assumed. Error bars indicate standard error of the mean (SEM) unless otherwise stated.

Results:

Expression of cathepsin B in 4T1.2 spontaneous bone metastasis mimics that of the human disease. To support a role for cathepsin B in bone metastasis, we evaluated protein levels in a cohort of human primary tumors (n=10) and bone metastases (n=5). In agreement with previous reports (15, 29), cathepsin B was detected in primary tumor and stromal cells (Figure 1A). Importantly, cathepsin B was also present in bone metastases. In all tumors, cathepsin B was expressed in tumor-associated stromal cells, including the local vasculature (Figure 1A) and over 60% of tumors expressed the protease in the tumor cells specifically. This staining pattern was consistent in all primary breast tumors and bone metastases examined.

To ensure that the cathepsin B expression in human tumors was similar in our 4T1.2 murine model (30), expression was assessed in primary tumors and matched metastases in bone. Cathepsin B was most intense at the periphery of the primary tumors, suggestive of a role in tumor invasion through the ECM. In spine metastases, levels were highest in tumor cells adjacent to bone and other stromal components (Figure 1B). This distribution of cathepsin B confirmed the value of the 4T1.2 model to dissect the function of cathepsin B in bone metastasis. Cathepsin B expression was also apparent in human and murine pulmonary metastases (Supplementary Figure 1).

Reduced cathepsin B in tumor cells lowers spontaneous metastasis to bone. To determine the functional consequences of lowering cathepsin B levels specifically in tumor cells, we stably transduced 4T1.2 cells with cathepsin B specific shRNA (CTSB kd) or control hairpins (4T1.2 BV). Stable knockdown of cathepsin B was verified by real-time RT-PCR (Supplementary Figure 2) and immunoblotting (Figure 2A). Inhibition of cathepsin B activity was also confirmed using a fluorometric assay that utilizes the selective cathepsin B substrate, Z-Arg-Arg-NHMec (25). Consistent

with decreased levels, cathepsin B activity in cell lysates was significantly lower in cathepsin B knockdown cells (Figure 2B and Supplementary Figure 3). In addition, intracellular and membrane associated cathepsin B staining was almost undetectable in the knockdown cell lines compared to the parental and base vector lines (Figure 2C). Importantly for proteolysis and metastasis assays, cathepsin B knockdown did not alter cell proliferation (Supplementary Figure 4).

To assess proteolytic activity in the 4T1.2 clonal pool, we used a recently established 3D *in vitro* confocal assay that mimics the architecture of the tumor microenvironment and enables imaging and quantification of proteolysis by living cells (26, 27). The degradation of collagen IV or collagen I by 4T1.2 parental cells, CTSB kd cells and cells treated with the cathepsin B selective inhibitor CA-074 (31) was assessed in the presence of the cathepsin B selective activity based probe (ABP) GB123. Cells were grown in reconstituted basement membrane (rBM) containing DQ-collagen IV or in collagen I containing DQ-collagen I. Images of the cells grown on rBM revealed tight three-dimensional spheroids (Figure 2D). In contrast, cells embedded in collagen I grew as monolayers (Figure 2E). 3D images of cell induced proteolysis are available online (supplementary materials, movie M1 to M6). Knockdown or inhibition of cathepsin B did not affect cellular morphology on either matrix. Importantly, GB123 staining confirmed a significant reduction in cysteine cathepsin activity in 3D cultures by CTSB knockdown or inhibition by CA-074 compared to parental 4T1.2 cells grown on either rBM or collagen I (Figure 2F and 2H respectively, $p<0.005$). Degradation of DQ-collagen IV was reduced by cathepsin B knockdown (Figure 2G) and to a greater extent by the CA-074 inhibitor. In addition, cathepsin B knockdown or inhibition in 4T1.2 cells led to a significant decrease in DQ-collagen I degradation (Figure 2I, $p<0.05$). Since collagen I is the predominant bone matrix protein, this is suggestive of a role for cathepsin B in bone degradation. These studies also support the use of small molecule cathepsin B inhibitors to reduce proteolysis.

We next injected parental 4T1.2, pooled 4T1.2 BV controls or CTSB kd cells into the mammary gland of Balb/c mice to test the impact of cathepsin B knockdown on metastasis. There was no difference in orthotopic tumor growth between the parental and CTSB kd groups (Figure 3A) even though knockdown was maintained (Figure 3B). Base vector control tumors expressed cathepsin B at the tumor edge as seen previously with the 4T1.2 tumors, whereas expression in CTSB kd tumor cells was negligible. Although cathepsin B knockdown did not reduce orthotopic mammary tumor growth, lung metastasis was significantly decreased in mice bearing CTSB kd tumors compared to 4T1.2 parental or 4T1.2 BV tumors (Figure 3C, $p<0.0001$). Although control 4T1.2 BV tumors grew at a slower rate than 4T1.2 parental tumors (Figure 3A), the metastatic burden at endpoint was not altered, hence 4T1.2 BV cells were appropriate controls for assessing the effect of cathepsin B knockdown on metastatic burden. The decrease in lung metastatic burden was confirmed by histology (Figure 3D). Of particular interest to this study, bone (spine) metastasis was also reduced dramatically in the CTSB kd group compared to 4T1.2 (Figure 3E, $p<0.005$) and base vector control (Figure 3E, $p<0.05$). Histological analysis of spine from 4T1.2 BV and CTSB kd tumor-bearing mice revealed tumor deposits in the control tissue that were not detectable in the spines of mice bearing CTSB kd tumors (Figure 3F).

Selective inhibition of cathepsin B suppresses distant metastasis. To test the therapeutic efficacy of cysteine protease inhibitors *in vivo*, we treated 4T1.2 tumor bearing mice with JPM-OEt (a broad spectrum cysteine protease inhibitor) (32) and the selective CA-074 inhibitor (31). Treatment of 4T1.2-tumor bearing mice with either inhibitor had no impact on primary tumor growth (Figure 4A and 4D). However, analysis of metastasis revealed a significant difference between these compounds. Treatment with the broad spectrum JPM-OEt inhibitor did not significantly reduce metastasis to lung or bone when compared to vehicle (Figure 4B and 4C). In contrast, CA-074 treatment significantly decreased

metastasis to lung (Figure 4E, $p<0.05$) and bone (Figure 4F, $p<0.05$). The effect of the inhibitors *in vivo* was further confirmed by histopathological analysis. Visible lung and spine metastatic nodules were observed in vehicle and JPM-OEt treatment groups, whereas tumors were undetectable in the CA-074 group (Figure 4H, 4I). Importantly, measurement of cysteine cathepsin B and L activity in primary tumor tissue lysates derived from mice treated with JPM-OEt and CA-074 revealed that both inhibitors reduced tumor cathepsin B activity significantly (Figure 4G, $p<0.005$), yet CA-074 was more effective. In contrast, only JPM-OEt inhibited cathepsin L activity (Figure 4G, $p<0.05$). Hence, the reduced efficacy of JPM-OEt could be due to the inhibition of other cysteine cathepsins that may have anti-tumorigenic functions (33) and/or due to a slightly reduced ability to suppress cathepsin B activity.

The CA-074 treatment studies were conducted from day 3 until metastasis was evident. This did not specifically allow assessment of the role of cathepsin B in the later steps of metastasis, preventing metastatic outgrowth once tumor cells had already lodged in distant tissues. We therefore performed a repeat CA-074 treatment experiment aimed at recapitulating a late-treatment setting. Primary tumors were removed and treatment began at day 20, a time when micrometastases can be detected in lung and bone. Analysis of metastatic burden revealed that there was a significant decrease in lung and overall bone metastases in this setting (Figure 5), revealing a role for cathespin B in late stages of metastatic spread.

Non-invasive *in vivo* imaging of cathepsin B activity in bone metastases. We used the activity based probe (ABP) GB123 to label active cysteine cathepsins *in vivo* in the presence and absence of cathepsin B inhibitors. Mice bearing 4T1.2 tumors were treated with CA-074 as described previously. To visualize cysteine cathepsin activity, GB123 was injected prior to *in vivo* imaging using fluorescence tomography (FMT2500, VisEn Medical). FMT whole body imaging allowed visualization of cysteine cathepsin activity at the site of orthotopic mammary tumors (Figure 6A). Cysteine cathepsin activity

was reduced in the CA-074 treated animals even though the tumors were similar in size, suggesting that the loss in GB123 fluorescence was due to decreased cathepsin B activity (Figure 6A). This loss was confirmed by *ex vivo* imaging of the tumors (Figure 6B), however was not significant and likely due to detection of other active cysteine cathepsins such as cathepsin L in the primary tumor by GB123. The cellular localization of cysteine cathepsin activity was additionally resolved by confocal microscopy (Figure 6C). Strongest activity was detected at the boundaries of the 4T1.2 tumors and this was lost in CA-074 treated mice. We next completed whole body scans of mice injected with both GB123 and Osteosense750 probes. Osteosense750 is a fluorescent diphosphonate imaging agent that detects active bone remodeling and hence allows bone visualization. Non-invasive whole body images of the spine region revealed GB123 signal in the spine of mice bearing 4T1.2 tumors that aligned with Osteosense750 signal (Figure 6D), and hence bone remodeling suggestive of an osteolytic tumor region. The GB123 signal was decreased in mice treated with CA-074 (Figure 6D). *Ex vivo* images of the spines confirmed this (Figure 6E, 6F). Quantitation of total GB123 fluorescence in spine, revealed a significant reduction in fluorescence in CA-074 treated compared to control treated mice (Figure 6G, $p < 0.05$).

Discussion:

Bone metastases occur in a high proportion of breast cancer patients with metastatic disease and are associated with severe morbidity and eventual mortality when visceral organs become involved. Dissecting the molecular mechanisms involved in tumor cell survival and outgrowth in bone is essential for the development of targeted therapies to reduce patient mortality. Here we report that tumor-derived cathepsin B is a key contributor to bone metastasis. Our data demonstrate for the first time that selective inhibition of cathepsin B using small molecule inhibitors significantly reduces metastasis and has therapeutic potential.

There are a number of critical steps required for growth of tumors in bone. This includes collaboration between the tumor cells themselves and the bone stroma for stimulating angiogenesis, invasion through the bone matrix and growth beyond the micrometastatic stage. Cathepsin B upregulation has been documented in several human cancers, including breast, prostate and melanoma (15, 34, 35). Our data demonstrate that cathepsin B has critical tumor-specific functions in breast cancer metastasis that are completely independent from primary tumor growth. We show that tumor cells themselves can directly degrade the major bone matrix protein collagen I and that cathepsin B is important, if not essential, in this process. Previous studies have implicated tumor cell cathepsin B in degradation of ECM proteins including fibronectin, laminin and collagen IV (36, 37). Additionally, and in support of our studies, inhibition of cathepsin B has been demonstrated to reduce collagen I degradation by prostate carcinoma cell lines (38), again suggestive of a tumor cell-specific role in bone lysis. Consistent with a role in invasion, we demonstrated a critical function of tumor-derived cathepsin B in metastasis in the 4T1.2 model. Although orthotopic tumor growth was not altered by cathepsin B knockdown, pulmonary and bone (spine) metastases were significantly reduced. As outgrowth of disseminated tumor cells into

macrometastases requires multiple steps including invasion through secondary tissues, preventing ECM degradation by cathepsin B inhibition is likely to reduce metastatic burden.

Cathepsin B has also been implicated in stromal cell-associated pro-tumorigenic functions. In breast cancer, this has been demonstrated using the MMTV-PyMT model where host-derived cathepsin B promotes lung metastasis (39). The expression of cathepsin B predominantly in tumor-infiltrating macrophages indicated that macrophage derived cathepsin B contributed to metastasis. The expression of cathepsin B in tumor-associated endothelial cells and macrophages has been associated with tumor progression via promotion of angiogenesis (17, 18). Cathepsin B has also been reported to be expressed in stromal fibroblasts and macrophages in colon and prostate cancers (40, 41). Taken together, cathepsin B has key roles in tumor progression, by invasion through the ECM and stimulation of angiogenesis. Our treatment of 4T1.2-tumor bearing mice with the selective small molecule cathepsin B inhibitor CA-074 enabled inhibition of both tumor and stromal cathepsin B and allowed assessment of the therapeutic benefit of inhibiting this protease *in vivo*. Consistent with cathepsin B transcript knockdown, treatment with CA-074 did not alter primary tumor growth yet suppression of metastasis was impressive. In fact, bone metastases could not be detected histologically in tumor-bearing mice treated with the inhibitor, an impressive result considering the aggressive nature of 4T1.2 tumors. Due to the role of cathepsin B in degradation of collagen IV and I, we hypothesized that metastasis inhibition was caused by decreased invasion at both the primary and metastatic site. Our results in a late treatment setting support a role for cathepsin B in metastasis post tumor cell arrest in distant tissues. Commencement of CA-074 treatment post primary tumor resection significantly decreased metastatic growth in lung and bone. The use of cathepsin inhibitors to decrease spontaneous breast cancer metastasis to bone from the mammary gland has not been reported previously. However, use of cathepsin K (42) (another cysteine cathepsin) and cathepsin G (43) (a serine protease) inhibitors have

been documented to suppress the formation and growth of breast cancer osteolytic lesions in experimental models of metastasis.

The therapeutic benefit of CA-074 treatment in the 4T1.2 model was in contrast to the broad spectrum inhibitor JPM-OEt, which did not decrease lung or spine metastases. In agreement with our studies, treatment of polyoma middle T oncogene-induced mammary carcinomas with JPM-OEt did not alter tumor weights and lung metastasis (33). Together, these studies reveal the importance of using specific targeted therapies *in vivo.* JPM-OEt targets several cysteine cathepsins, some of which could actually have tumor suppressive functions. For example, cathepsin L activity is decreased in highly metastatic 4T1.2 tumors compared to weakly or non-metastatic tumors (20) suggesting inhibitory effects of this protease on tumor progression, as has been suggested before in skin tumorigenesis (44). The importance of using specific protease inhibitors is clear from early clinical trials using MMP inhibitors where inhibition of certain MMPs actually has deleterious effects in patients (45,46). These studies highlight the significant effort needed to determine which specific proteases contribute to advanced disease progression before potential drugs can be tested in the clinic.

Current treatments available for patients with bone metastasis are aimed primarily at reducing the morbidity associated with bone lysis, a hallmark of breast cancer bone disease. One target of such treatments is cathepsin K. Cathepsin K is expressed predominantly in osteoclasts where it is secreted and has a key role in bone proteolysis, including degradation of collagen I, osteonectin and osteopontin (47). The potential role of cathepsin K in osteolytic bone tumors is evident from its expression in tumor associated osteoclasts (48), in breast and prostate metastases in bone and in giant cell tumor of bone (49). Cathepsin K inhibitors block bone resorption (50), reducing the pain associated with osteolytic disease, and in turn slow the growth of bone tumors. However, as with the use of

bisphosphonates that also suppress osteolysis, treatment is not curative. Therefore, an ideal treatment (or combination of treatments) is one that targets both the tumor cell and the associated stromal populations that promote osteolysis, angiogenesis and tumor growth. The fact that cathepsin B has essential roles throughout the metastatic cascade, in tumor and stromal cells, suggests that combining cathepsin B inhibitors with conventional therapies may be of clinical value.

Acknowledgements:

This work was supported by the US Department of Defense BCRP Concept Award W81XWH-05-1-0444 (to BSP), National Health and Medical Research Council (NHMRC) grant 509325 (BSP, RLA, MSB) and Career Development Award 566553 (BSP)**,** National Breast Cancer Foundation (Australia) fellowship (RLA), NHMRC postgraduate scholarship ID 466645 (to NPW)**.** This work was also supported, in part, by the National Institutes of Health [R01CA131990 (BFS)].

References

1. American Cancer Society. Cancer Facts & Figures 2010; 2010.

2. Turk V, Kos J, Turk B. Cysteine cathepsins (proteases)--on the main stage of cancer? Cancer Cell. 2004 May;5(5):409-10.

3. Brix K, Dunkhorst A, Mayer K, Jordans S. Cysteine cathepsins: cellular roadmap to different functions. Biochimie. 2008 Feb;90(2):194-207.

4. Conus S, Simon HU. Cathepsins: key modulators of cell death and inflammatory responses. Biochem Pharmacol. 2008 Dec 1;76(11):1374-82.

5. Tardy C, Codogno P, Autefage H, Levade T, Andrieu-Abadie N. Lysosomes and lysosomal proteins in cancer cell death (new players of an old struggle). Biochim Biophys Acta. 2006 Apr;1765(2):101-25.

6. Zavasnik-Bergant T, Turk B. Cysteine proteases: destruction ability versus immunomodulation capacity in immune cells. Biol Chem. 2007 Nov;388(11):1141-9.

7. Troen BR. The role of cathepsin K in normal bone resorption. Drug News Perspect. 2004 Jan-Feb;17(1):19-28.

8. Gocheva V, Joyce JA. Cysteine cathepsins and the cutting edge of cancer invasion. Cell Cycle. 2007 Jan 1;6(1):60-4.

9. Mohamed MM, Sloane BF. Cysteine cathepsins: multifunctional enzymes in cancer. Nat Rev Cancer. 2006 Oct;6(10):764-75.

10. Vasiljeva O, Reinheckel T, Peters C, Turk D, Turk V, Turk B. Emerging roles of cysteine cathepsins in disease and their potential as drug targets. Curr Pharm Des. 2007;13(4):387-403.

11. Joyce JA, Hanahan D. Multiple roles for cysteine cathepsins in cancer. Cell Cycle. 2004 Dec;3(12):1516-619.

12. Lankelma JM, Voorend DM, Barwari T, et al. Cathepsin L, target in cancer treatment? Life Sci. 2010 Feb 13;86(7-8):225-33.

13. Jain M, Bakhshi S, Shukla AA, Chauhan SS. Cathepsins B and L in peripheral blood mononuclear cells of pediatric acute myeloid leukemia: potential poor prognostic markers. Ann Hematol. 2010 Jun 22.

14. Lah TT, Kalman E, Najjar D, et al. Cells producing cathepsins D, B, and L in human breast carcinoma and their association with prognosis. Hum Pathol. 2000 Feb;31(2):149-60.

15. Nouh MA, Mohamed MM, El-Shinawi M, et al. Cathepsin B: A potential prognostic marker for inflammatory breast cancer. J Transl Med. 2011 Jan 3;9(1):1.

16. Vasiljeva O, Korovin M, Gajda M, et al. Reduced tumor cell proliferation and delayed development of high-grade mammary carcinomas in cathepsin B-deficient mice. Oncogene. 2008 Mar 17.

17. Sevenich L, Werner F, Gajda M, et al. Transgenic expression of human cathepsin B promotes progression and metastasis of polyoma-middle-T-induced breast cancer in mice. Oncogene. 2010 Sep 6.

18. Joyce JA, Baruch A, Chehade K, et al. Cathepsin cysteine proteases are effectors of invasive growth and angiogenesis during multistage tumorigenesis. Cancer Cell. 2004 May;5(5):443-53.

19. Bell-McGuinn KM, Garfall AL, Bogyo M, Hanahan D, Joyce JA. Inhibition of cysteine cathepsin protease activity enhances chemotherapy regimens by decreasing tumor growth and invasiveness in a mouse model of multistage cancer. Cancer Res. 2007 Aug 1;67(15):7378-85.

20. Parker BS, Ciocca DR, Bidwell BN, et al. Primary tumor expression of the cysteine cathepsin inhibitor Stefin A inhibits distant metastasis in breast cancer. The Journal of pathology. 2008 Feb;214(3):337-46.

21. Eckhardt BL, Parker BS, van Laar RK, et al. Genomic analysis of a spontaneous model of breast cancer metastasis to bone reveals a role for the extracellular matrix. Mol Cancer Res. 2005 Jan;3(1):1-13.

22. Sinha AA, Quast BJ, Wilson MJ, et al. Prediction of pelvic lymph node metastasis by the ratio of cathepsin B to stefin A in patients with prostate carcinoma. Cancer. 2002 Jun 15;94(12):3141-9.

23. Strojnik T, Zajc I, Bervar A, et al. Cathepsin B and its inhibitor stefin A in brain tumors. Pflugers Arch. 2000;439(3 Suppl):R122-3.

24. Moin K, Day NA, Sameni M, Hasnain S, Hirama T, Sloane BF. Human tumor cathepsin B. Comparison with normal liver cathepsin B. Biochem J. 1992 Jul 15;285 (Pt 2):427-34.

25. Cavallo-Medved D, Rudy D, Blum G, Bogyo M, Caglic D, Sloane BF. Live-cell imaging demonstrates extracellular matrix degradation in association with active cathepsin B in caveolae of endothelial cells during tube formation. Exp Cell Res. 2009 Apr 15;315(7):1234-46.

26. Jedeszko C, Sameni M, Olive MB, Moin K, Sloane BF. Visualizing protease activity in living cells: from two dimensions to four dimensions. Curr Protoc Cell Biol. 2008 Jun;Chapter 4:Unit 4 20.

27. Sameni M, Cavallo-Medved D, Dosescu J, et al. Imaging and quantifying the dynamics of tumor-associated proteolysis. Clin Exp Metastasis. 2009;26(4):299-309.

28. Blum G, von Degenfeld G, Merchant MJ, Blau HM, Bogyo M. Noninvasive optical imaging of cysteine protease activity using fluorescently quenched activity-based probes. Nat Chem Biol. 2007 Oct;3(10):668-77.

29. Berdowska I. Cysteine proteases as disease markers. Clin Chim Acta. 2004 Apr;342(1-2):41-69.

30. Lelekakis M, Moseley JM, Martin TJ, et al. A novel orthotopic model of breast cancer metastasis to bone. Clin Exp Metastasis. 1999 Mar;17(2):163-70.

31. Murata M, Miyashita S, Yokoo C, et al. Novel epoxysuccinyl peptides. Selective inhibitors of cathepsin B, in vitro. FEBS Lett. 1991 Mar 25;280(2):307-10.

32. Meara JP, Rich DH. Mechanistic studies on the inactivation of papain by epoxysuccinyl inhibitors. J Med Chem. 1996 Aug 16;39(17):3357-66.

33. Schurigt U, Sevenich L, Vannier C, et al. Trial of the cysteine cathepsin inhibitor JPM-OEt on early and advanced mammary cancer stages in the MMTV-PyMT-transgenic mouse model. Biol Chem. 2008 Aug;389(8):1067-74.

34. Matarrese P, Ascione B, Ciarlo L, et al. Cathepsin B inhibition interferes with metastatic potential of human melanoma: an in vitro and in vivo study. Mol Cancer. 2010;9:207.

35. Qian J, Bostwick DG, Iczkowski KA, et al. Characterization of prostate cancer in needle biopsy by cathepsin B, cell proliferation and DNA ploidy. Anticancer Res. 2010 Mar;30(3):719-25.

36. Buck MR, Karustis DG, Day NA, Honn KV, Sloane BF. Degradation of extracellular-matrix proteins by human cathepsin B from normal and tumor tissues. Biochem J. 1992 Feb 15;282 (Pt 1):273-8.

37. Premzl A, Zavasnik-Bergant V, Turk V, Kos J. Intracellular and extracellular cathepsin B facilitate invasion of MCF-10A neoT cells through reconstituted extracellular matrix in vitro. Exp Cell Res. 2003 Feb 15;283(2):206-14.

38. Podgorski I, Linebaugh BE, Sameni M, et al. Bone microenvironment modulates expression and activity of cathepsin B in prostate cancer. Neoplasia. 2005 Mar;7(3):207-23.

39. Vasiljeva O, Papazoglou A, Kruger A, et al. Tumor cell-derived and macrophage-derived cathepsin B promotes progression and lung metastasis of mammary cancer. Cancer Res. 2006 May 15;66(10):5242-50.

40. Campo E, Munoz J, Miquel R, et al. Cathepsin B expression in colorectal carcinomas correlates with tumor progression and shortened patient survival. Am J Pathol. 1994 Aug;145(2):301-9.

41. Fernandez PL, Farre X, Nadal A, et al. Expression of cathepsins B and S in the progression of prostate carcinoma. Int J Cancer. 2001 Jan 20;95(1):51-5.

42. Le Gall C, Bellahcene A, Bonnelye E, et al. A cathepsin k inhibitor reduces breast cancer induced osteolysis and skeletal tumor burden. Cancer Res. 2007 Oct 15;67(20):9894-902.

43. Wilson TJ, Nannuru KC, Futakuchi M, et al. Cathepsin G enhances mammary tumor-induced osteolysis by generating soluble receptor activator of nuclear factor-kappaB ligand. Cancer Res. 2008 Jul 15;68(14):5803-11.

44. Benavides F, Perez C, Blando J, et al. Protective role of cathepsin L in mouse skin carcinogenesis. Mol Carcinog. 2011 May 2.

45. Fingleton B. Matrix metalloproteinase inhibitors for cancer therapy:the current situation and future prospects. Expert Opin Ther Targets. 2003 Jun;7(3):385-97.

46. Overall CM, Kleifeld O. Towards third generation matrix metalloproteinase inhibitors for cancer therapy. Br J Cancer. 2006 Apr 10;94(7):941-6.

47. Papachristou DJ, Basdra EK, Papavassiliou AG. Bone metastases: Molecular mechanisms and novel therapeutic interventions. Med Res Rev. 2010 Sep 3.

48. Salminen-Mankonen HJ, Morko J, Vuorio E. Role of cathepsin K in normal joints and in the development of arthritis. Curr Drug Targets. 2007 Feb;8(2):315-23.

49. Lindeman JH, Hanemaaijer R, Mulder A, et al. Cathepsin K is the principal protease in giant cell tumor of bone. Am J Pathol. 2004 Aug;165(2):593-600.

50. Bromme D, Lecaille F. Cathepsin K inhibitors for osteoporosis and potential off-target effects. Expert Opin Investig Drugs. 2009 May; 18(5):585-600.

Figure Legends:

Figure 1

Cathepsin B levels in human breast tumors (A) and mouse 4T1.2 tumors (B). Sections were immunostained for cathepsin B or with rabbit Ig isotype control antibodies and visualized with DAB. All tissues were counterstained with hematoxylin. Arrow indicates vasculature. Scale bar represents 50 μm.

Figure 2

Cathepsin B knockdown in 4T1.2 tumor cells reduces the degradation of DQ-collagen. (A) Western blot detection of cathepsin B protein expression in 4T1.2 parental cells, pooled 4T1.2 BV and CTSB kd clones. (B) Cathepsin B activity. (C) Cathepsin B expression (green) in 4T1.2 cells (blue). Frame captures of 3D reconstructions of parental 4T1.2 and CTSB kd tumor cells (cyan nuclei staining) grown on (D) rBM containing 25 μg/ml DQ-collagen IV (green) or (E) collagen I containing 25 μg/ml DQcollagen I (green), in the presence of1 μM GB123 (red), along with 4T1.2 cells treated with 20 μM Ca-074. (F) Quantification of GB123 cathepsin activity and (G) DQ-collagen IV degradation products from panel D. (H) Quantification of GB123 cathepsin activity and (I) DQ-collagen I degradation products from panel E. *$p < 0.05$, **$p< 0.005$, ****$p< 0.0001$.

Figure 3

Cathepsin B knockdown reduces spontaneous metastasis to lung and bone. (A) Primary tumor volumes. Error bar represents SEM. (B) IHC detection of cathepsin B in primary tumors from 4T1.2 BV and CTSB kd tumor bearing mice. (C) RT-QPCR detection of tumor burden in lung (using hygromycin-tagged 4T1.2 cells). Relative tumor burden compares tumor cell hygromycin DNA signal to that of vimentin expression in all murine cells. (D) H&E stained lung sections of 4T1.2 BV and CTSB kd

tumor-bearing mice. (E) RT-QPCR detection of tumor burden in spine (using hygromycin-tagged 4T1.2 cells). (F) H&E stained spine sections of 4T1.2 BV and CTSB kd tumor-bearing mice. T denotes tumor region. Scale bar represents 50 μm. *p<0.05, **p<0.005, ****p<0.0001

Figure 4

Treatment of tumor bearing mice with cathepsin inhibitors. Mice bearing 4T1.2 tumors were treated with 50 mg/kg JPM-OEt, CA-074, or vehicle (5% DMSO/Saline), three days post tumor inoculation. Primary tumor volumes over 28 days in, (A) JPM-OEt and (D) CA-074 treatment groups. Error bar represents SEM (n=20). RT-QPCR of genomic DNA containing the tumor specific hygromycin reporter gene was used for detection of tumor burden in lung (B and E) and spine (C and F) of JPM-OEt and CA-074 treated mice respectively. Relative tumor burden is a measure of the hygromycin signal relative to vimentin signal that is present in all cells. (G) Cathepsin B and L activity in vehicle, JPM-OEt and CA-074 treated primary tumors. H&E stained (H) lung and (I) spine sections of vehicle, JPM-OEt and CA-074 treated 4T1.2 tumor-bearing mice. T denotes tumor region. Scale bar represents 50μm. *p< 0.05, **p< 0.005, ***p ≤ 0.0005.

Figure 5

Late stage treatment of mice bearing 4T1.2 tumors with CA-074. 5 days after primary tumor resection, mice were treated daily intra peritoneally with 50 mg/kg CA-074, or vehicle (5% DMSO/Saline). RT-QPCR of genomic DNA containing the tumor specific hygromycin reporter gene was used for detection of tumor burden in lung (A), spine (B), femur (C). (D) Combined QPCR detection in spine and femurs. Error bar represents SEM, *p≤0.05.

Figure 6

In vivo imaging of cathepsin B activity in tumor burdened mice. (A) Fluorescence images of live mice bearing 4T1.2 tumors treated with vehicle or CA-074 followed by GB123. (B) Total tumor fluorescence in tumors excised 24 hours after probe injection and imaged *ex vivo* using the FMT2500 system. (C) Histology of vehicle and CA-074 treated mammary tumor tissues from A. Nuclei were visualised with DAPI. (D) Fluorescence spinal images of live mice bearing 4T1.2 tumors treated with vehicle or CA-074 followed by GB123 and osteosense 750. (E) Total metastases fluorescence in spines excised 24 hours after probe injection and imaged *ex vivo*. (F) Histology of vehicle and CA-074 treated spine tissues from D. Tissues were stained with DAPI, and images were taken using a 60x objective. Red indicates GB123 fluorescence; blue indicates DAPI. The colorimetric scale bars indicate nm of fluorescence. (G) Quantitation of total GB123 metastases fluorescence in vehicle and CA-074 treated spines using the FMT2500 system. Mean fluorescence with standard error is shown. *$p<0.05$. Scale bar represents 50μm.

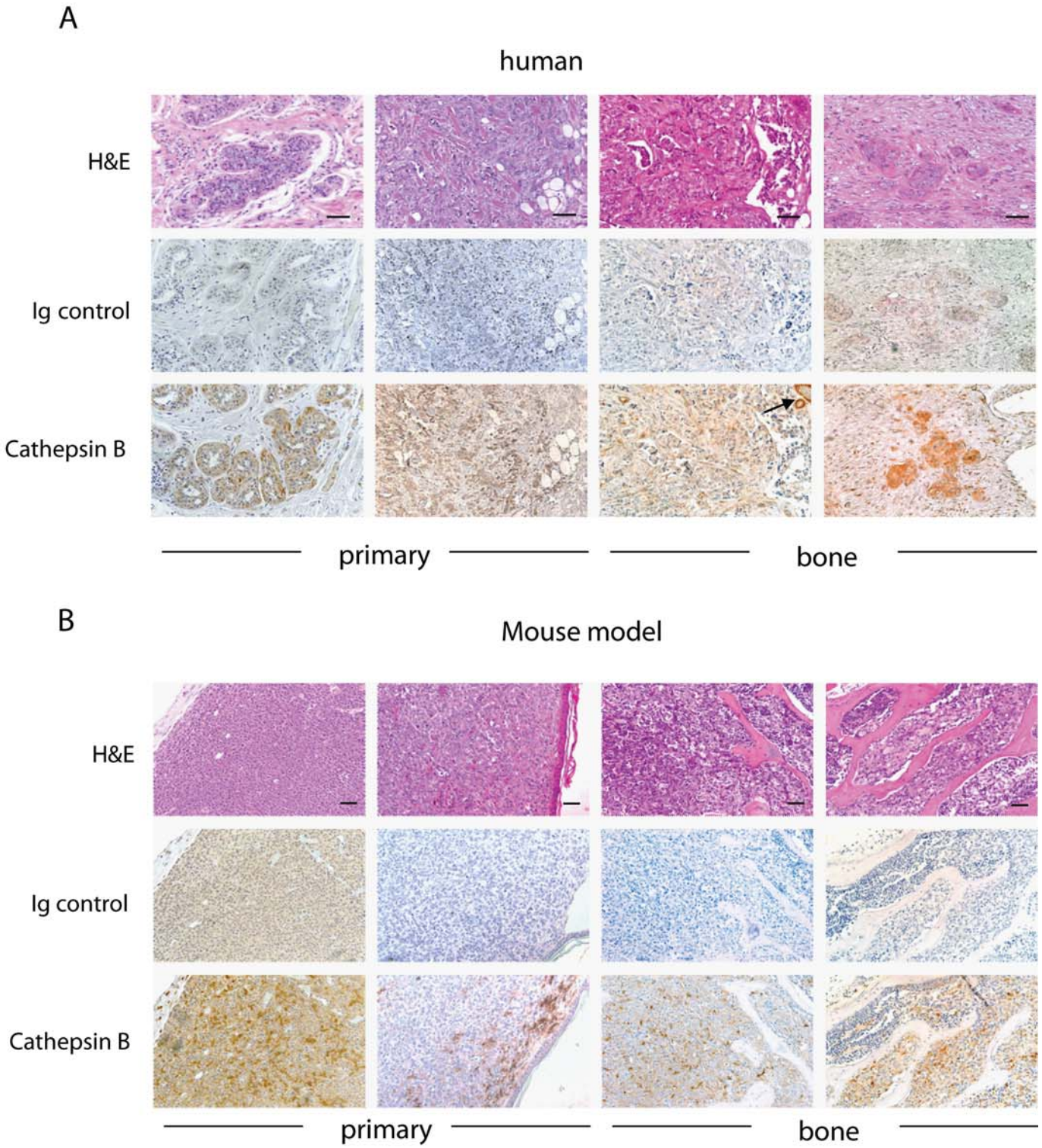

Figure 1

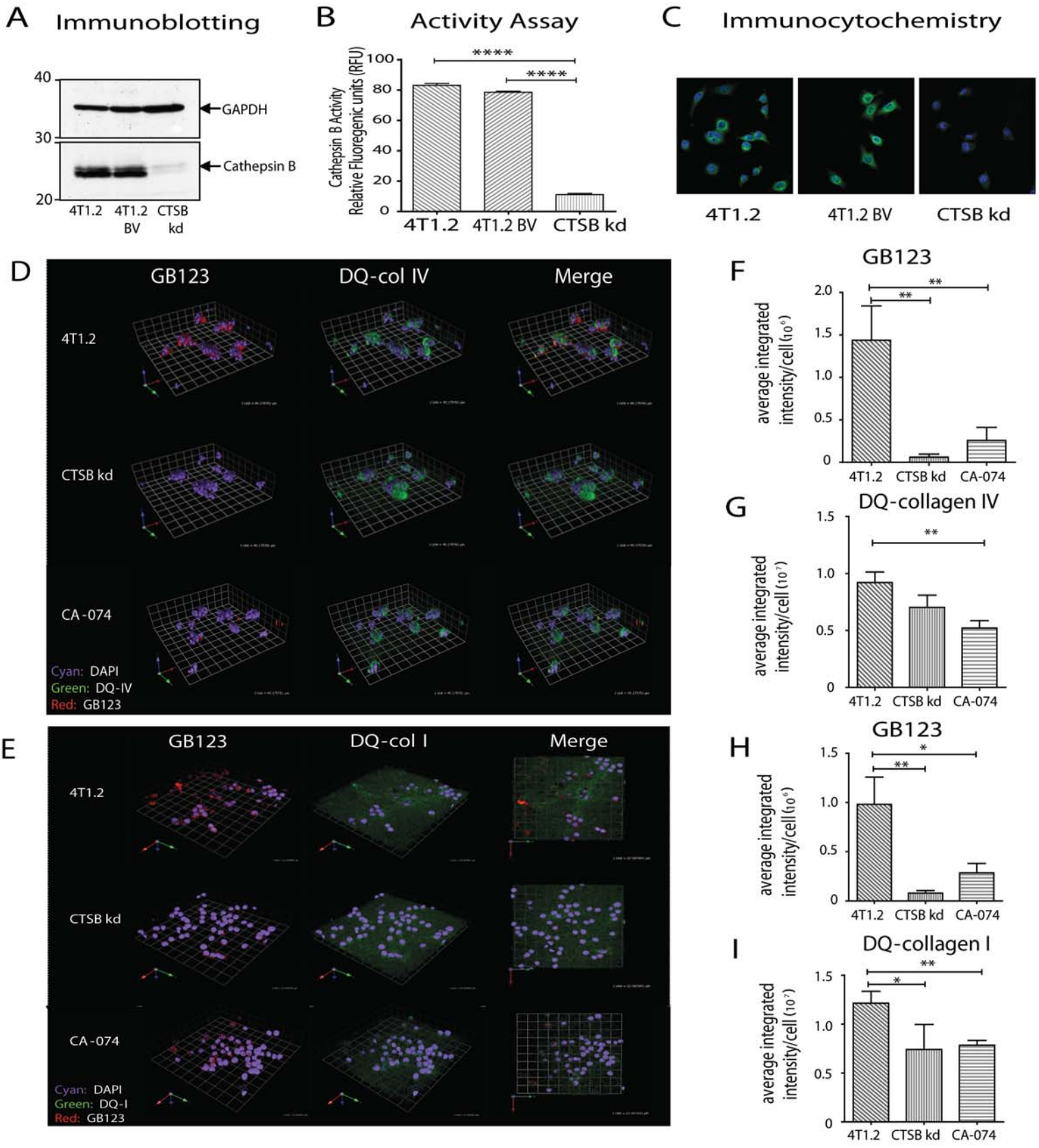

Figure 2

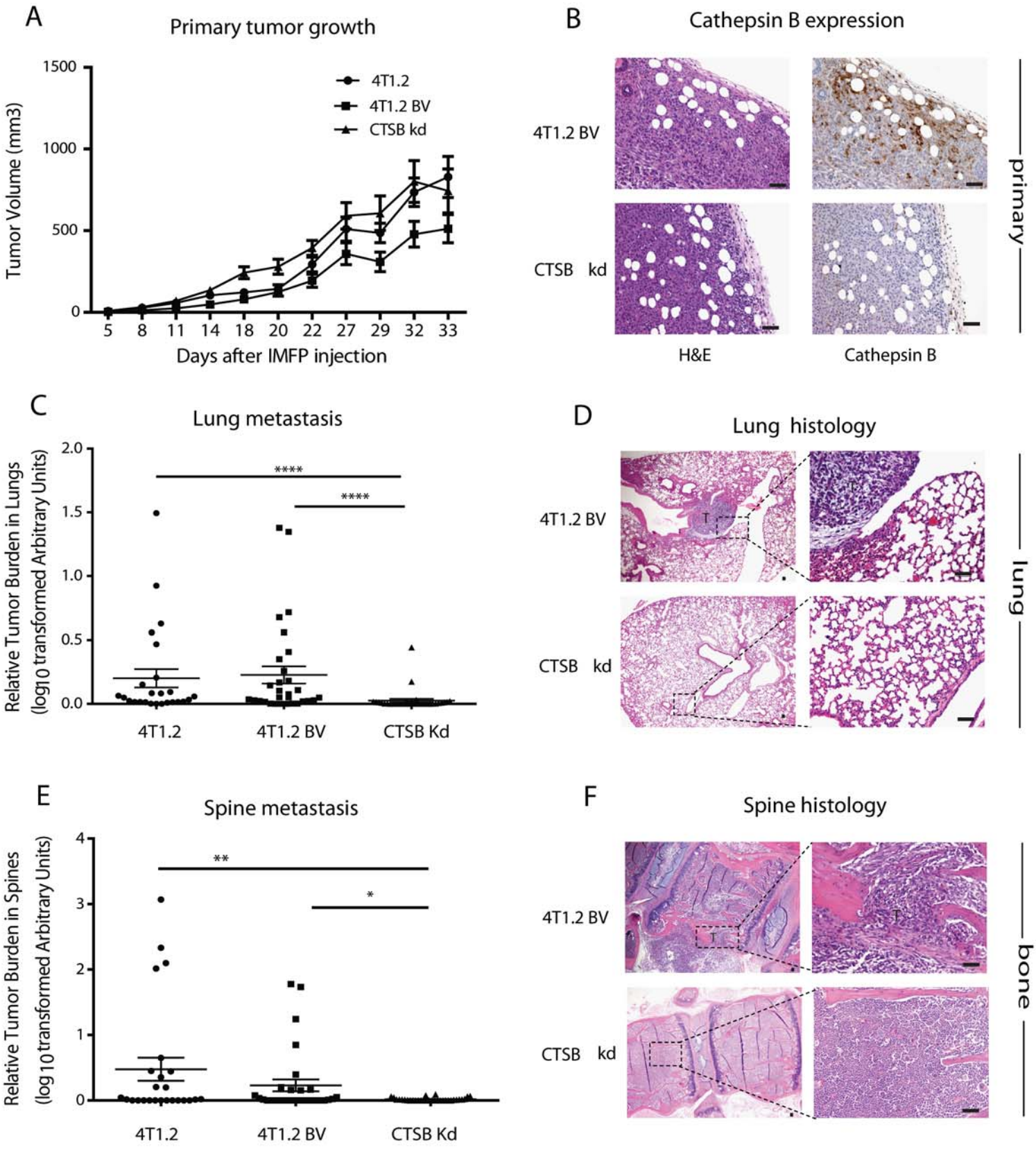

Figure 3

Author Manuscript Published OnlineFirst on January 19, 2012; DOI:10.1158/0008-5472.CAN-11-2759
Author manuscripts have been peer reviewed and accepted for publication but have not yet been edited.

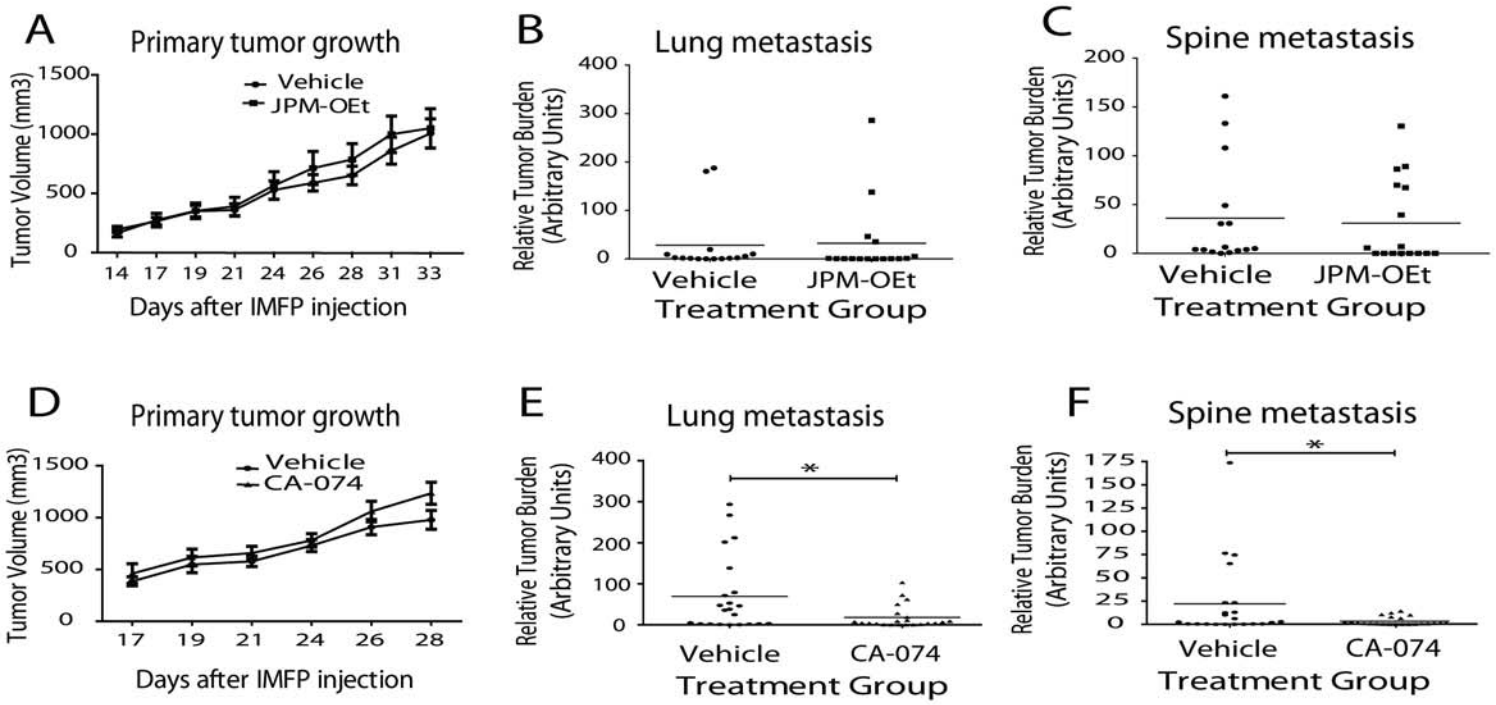

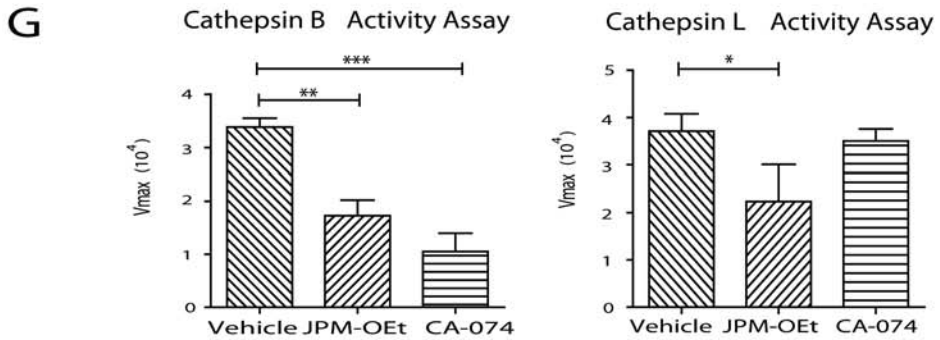

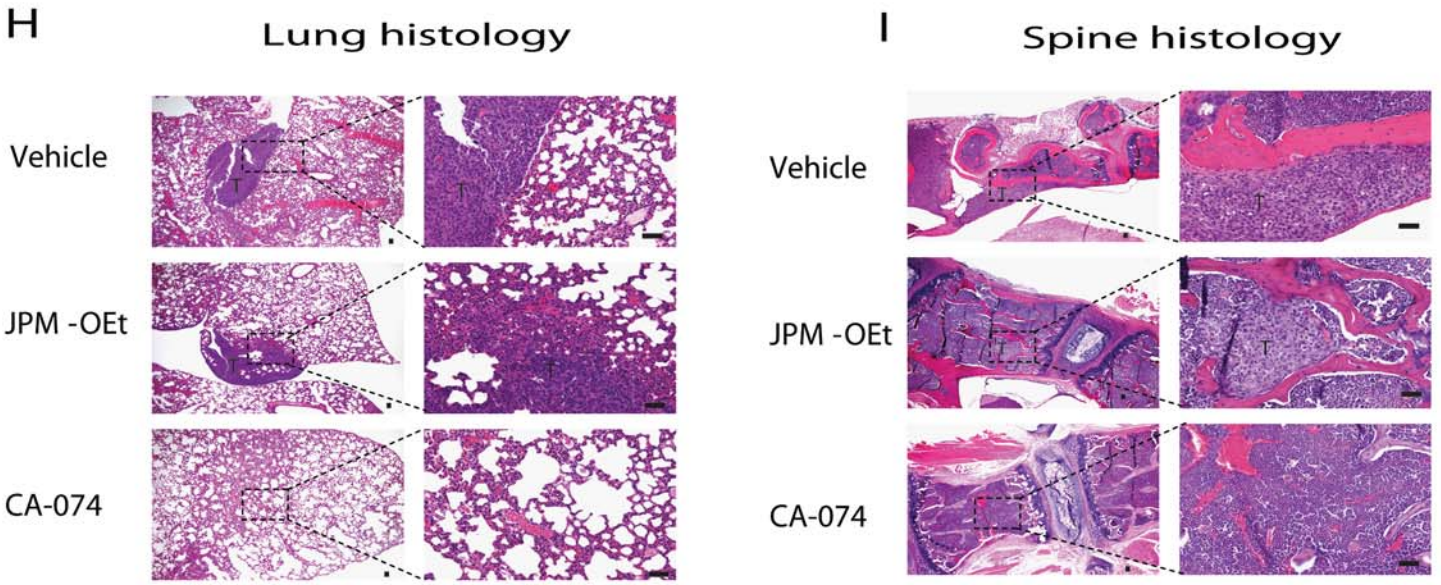

Figure 4

Author Manuscript Published OnlineFirst on January 19, 2012; DOI:10.1158/0008-5472.CAN-11-2759
Author manuscripts have been peer reviewed and accepted for publication but have not yet been edited.

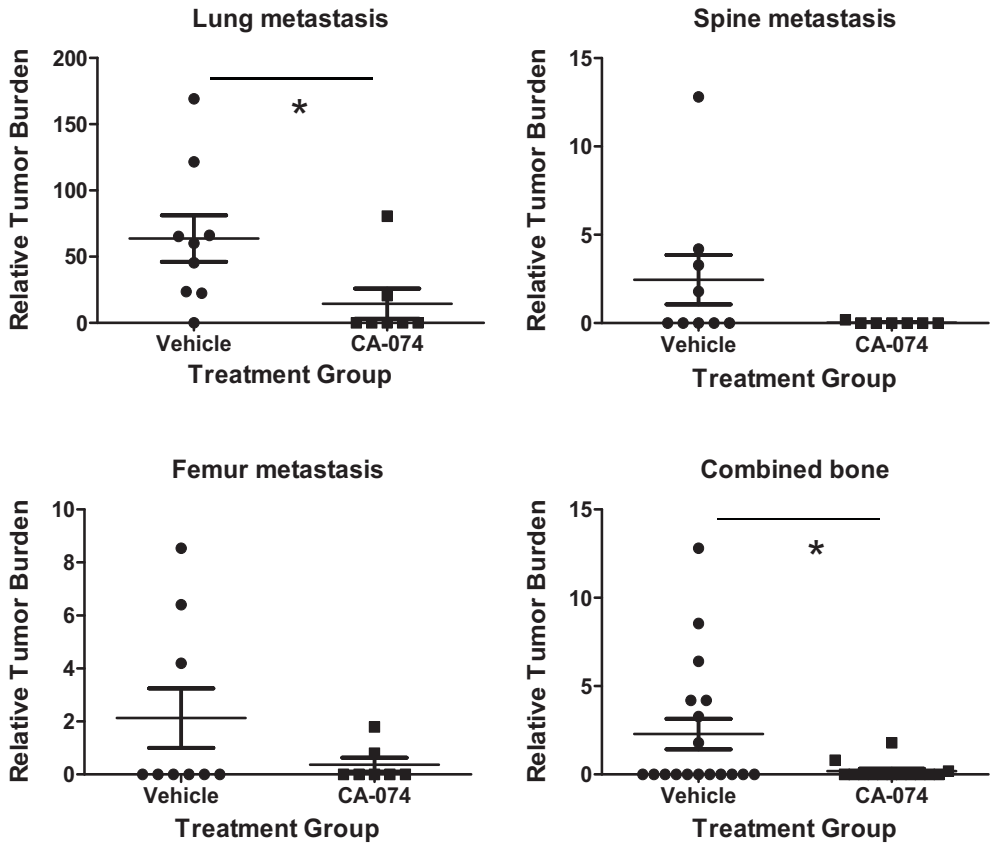

Figure 5

Author Manuscript Published OnlineFirst on January 19, 2012; DOI:10.1158/0008-5472.CAN-11-2759
Author manuscripts have been peer reviewed and accepted for publication but have not yet been edited.

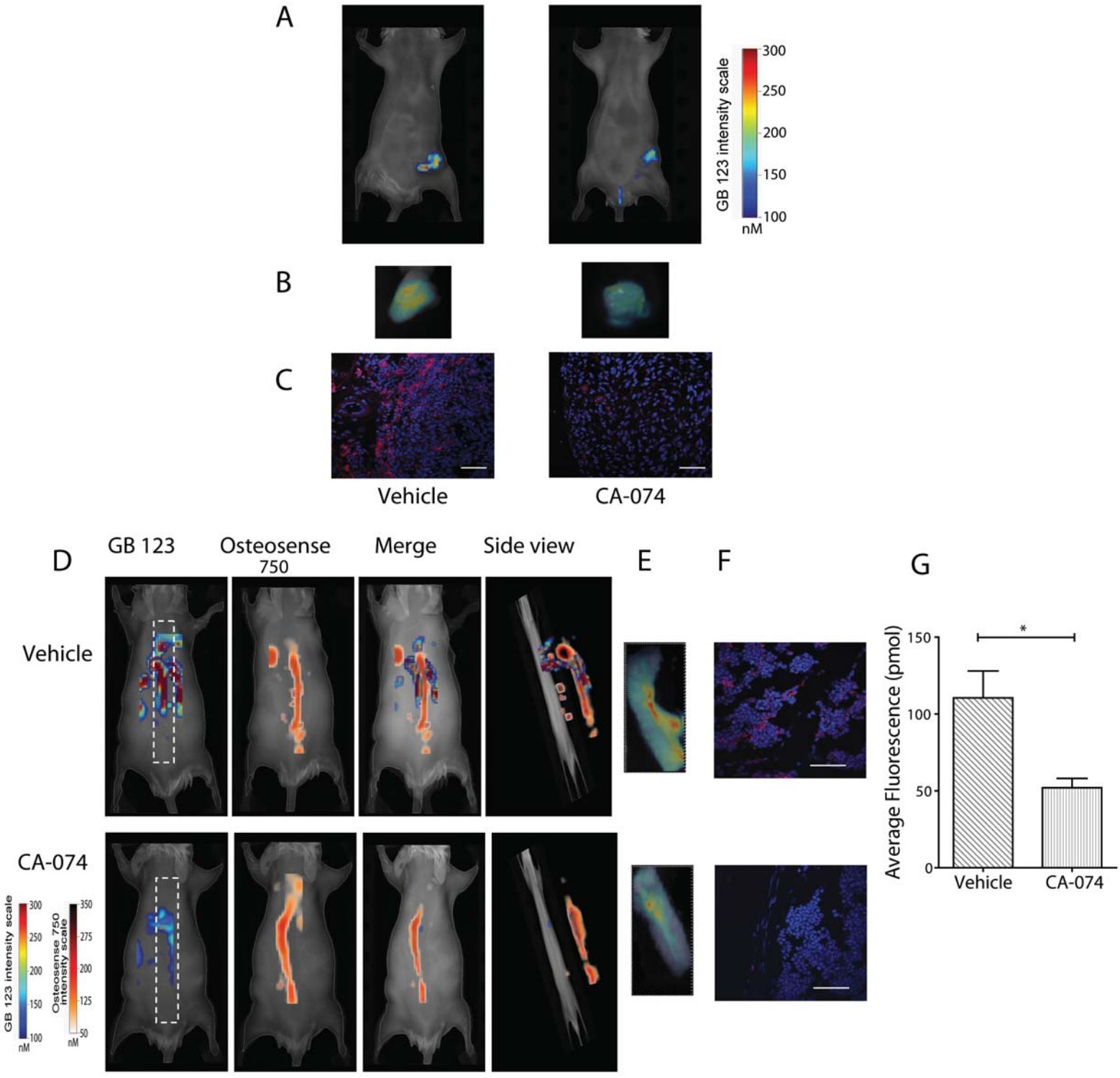

Figure 6